Double-clad hollow core photonic crystal fiber for coherent Raman endoscope

S. Brustlein, P. Berto, R. Hostein, Patrick Ferrand, C. Billaudeau, D. Marguet, A. Muir, J. Knight, H. Rigneault

Double-clad hollow core photonic crystal fiber for coherent Raman endoscope

Sophie Brustlein,[1,2,3] Pascal Berto,[1,2,3] Richard Hostein,[1,2,3] Patrick Ferrand,[1,2,3] Cyrille Billaudeau,[4,5,6] Didier Marguet,[4,5,6] Alistair Muir,[7] Jonathan Knight,[7] and Hervé Rigneault[1,2,3,*]

[1] *Aix-Marseille Université, Institut Fresnel, Campus de Saint Jérôme, F-13013 Marseille, France*
[2] *Ecole Centrale Marseille, Institut Fresnel, Campus de St Jérôme, F-13013 Marseille, France*
[3] *CNRS, Institut Fresnel, Campus de St Jérôme, F-13013 Marseille, France*
[4] *Centre d'Immunologie de Marseille-Luminy, INSERM, UMR-S 631, F-13009 Marseille, France*
[5] *CNRS, UMR 6102, F-13009 Marseille, France*
[6] *Université de la Méditerranée, UM 631, F-13009 Marseille, France*
[7] *Centre for Photonics and Photonic Materials, Department of Physics, University of Bath, Claverton Down, Bath, BA2 7AY, UK*
**herve.rigneault@fresnel.fr*

Abstract: Performing label free coherent anti-Stokes Raman scattering (CARS) and stimulated Raman scattering (SRS) in endoscope imaging is a challenge, with huge potential clinical benefit. To date, this goal has remained inaccessible because of the inherent coherent Raman noise that is generated in the fiber itself. By developing double-clad hollow core photonic crystal fiber, we demonstrate coherent anti-Stokes Raman scattering and stimulated Raman scattering in an 'endoscope-like' scheme. Both the excitation beams and the collected CARS and SRS signals travel through the same fiber. No CARS and SRS signals are generated within the hollow core fiber even for temporally overlapping pump and Stokes beams, leading to excellent image quality. The CARS and SRS signals generated in the sample are coupled back into a high numerical aperture multimode cladding surrounding the central photonic crystal cladding. We demonstrate this scheme by imaging molecular vibrational bonds of organic crystal deposited on a glass surface.

OCIS codes: (060.5295) Photonic crystal fibers; (180.4315) Nonlinear microscopy; (190.4380) Nonlinear optics, four-wave mixing; (300.6230) Spectroscopy, coherent anti-Stokes Raman scattering.

References and links

1. A. Zumbusch, G. R. Holtom, and X. S. Xie, "Vibrationnal microscopy using coherent anti-Stokes Raman scattering," Phys. Rev. Lett. **82**, 4014–4017 (1999).
2. C. L. Evans and X. S. Xie, "Coherent anti-stokes Raman scattering microscopy: chemical imaging for biology and medicine," Annu Rev Anal Chem (Palo Alto Calif) **1**(1), 883–909 (2008).
3. C. W. Freudiger, W. Min, B. G. Saar, S. Lu, G. R. Holtom, C. He, J. C. Tsai, J. X. Kang, and X. S. Xie, "Label-free biomedical imaging with high sensitivity by stimulated Raman scattering microscopy," Science **322**(5909), 1857–1861 (2008).
4. P. Nandakumar, A. Kovalev, and A. Volkmer, "Vibrational imaging based on stimulated Raman scattering microscopy," N. J. Phys. **11**(3), 033026 (2009).
5. X. S. Xie, J. Yu, and W. Y. Yang, "Living cells as test tubes," Science **312**(5771), 228–230 (2006).
6. E. Gratton and M. Digman, "One photon up, one photon down," Nat. Biotechnol. **27**(2), 147–148 (2009).
7. F. Légaré, C. L. Evans, F. Ganikhanov, and X. S. Xie, "Towards CARS Endoscopy," Opt. Express **14**, 4427–4432 (2006), *http://www.opticsinfobase.org/oe/abstract.cfm?URI=oe-14-10-4427*.
8. M. Balu, G. Liu, Z. Chen, B. J. Tromberg, and E. O. Potma, "Fiber delivered probe for efficient CARS imaging of tissues," Opt. Express **18**(3), 2380–2388 (2010), http://www.opticsinfobase.org/oe/abstract.cfm?URI=oe-18-3-2380.
9. B. A. Flusberg, E. D. Cocker, W. Piyawattanametha, J. C. Jung, E. L. M. Cheung, and M. J. Schnitzer, "Fiber-optic fluorescence imaging," Nat. Methods **2**(12), 941–950 (2005).
10. R. F. Cregan, B. J. Mangan, J. C. Knight, T. A. Birks, P. St. J. Russell, P. J. Roberts, and D. C. Allan, "Single-Mode Photonic Band Gap Guidance of Light in Air," Science **285**(5433), 1537–1539 (1999).

#146014 - $15.00 USD Received 20 Apr 2011; revised 7 Jun 2011; accepted 7 Jun 2011; published 14 Jun 2011

11. G. Humbert, J. Knight, G. Bouwmans, P. Russell, D. Williams, P. Roberts, and B. Mangan, "Hollow core photonic crystal fibers for beam delivery," Opt. Express **12**(8), 1477–1484 (2004), http://www.opticsinfobase.org/oe/abstract.cfm?URI=oe-12-8-1477.
12. J. X. Cheng, A. Volkmer, and X. S. Xie, "Theoretical and experimental characterization of coherent anti-Stokes Raman scattering microscopy," J. Opt. Soc. Am. B **19**(6), 1363–1375 (2002).
13. M. T. Myaing, J. Y. Ye, T. B. Norris, T. Thomas, J. R. Baker, Jr., W. J. Wadsworth, G. Bouwmans, J. C. Knight, and P. S. Russell, "Enhanced two-photon biosensing with double-clad photonic crystal fibers," Opt. Lett. **28**(14), 1224–1226 (2003).
14. L. Fu, X. Gan, and M. Gu, "Nonlinear optical microscopy based on double-clad photonic crystal fibers," Opt. Express **13**(14), 5528–5534 (2005), http://www.opticsinfobase.org/oe/abstract.cfm?URI=oe-13-14-5528.
15. F. Benabid, "Hollow-core photonic bandgap fiber: new light guidance for new science and technology," Philos. T. Roy. Soc. A. **364**(1849), 3439–3462 (2006).
16. S. Brustlein, P. Ferrand, N. Walther, S. Brasselet, C. Billaudeau, D. Marguet, and H. Rigneault, "Optical parametric oscillator-based light source for coherent Raman scattering microscopy: practical overview," J. Biomed. Opt. **16**(2), 021106 (2011).
17. M. Y. Jeong, H. M. Kim, S. J. Jeon, S. Brasselet, and B. R. Cho, "Octupolar Films with Significant Second-Harmonic Generation," Adv. Mater. (Deerfield Beach Fla.) **19**(16), 2107–2111 (2007).
18. T. Andersen, K. Hilligsøe, C. Nielsen, J. Thøgersen, K. Hansen, S. Keiding, and J. Larsen, "Continuous-wave wavelength conversion in a photonic crystal fiber with two zero-dispersion wavelengths," Opt. Express **12**(17), 4113–4122 (2004), http://www.opticsinfobase.org/oe/abstract.cfm?URI=oe-12-17-4113.
19. B. G. Saar, C. W. Freudiger, J. Reichman, C. M. Stanley, G. R. Holtom, and X. S. Xie, "Video-rate molecular imaging in vivo with stimulated Raman scattering," Science **330**(6009), 1368–1370 (2010).

1. Introduction

Since its first report in 1999 [1], coherent anti-Stokes Raman scattering (CARS) microscopy has made a great impact in cell biology and biomedical imaging [2] because it provides a label-free contrast mechanism compatible with living samples. Quite recently the inherent nonresonant background present in CARS has been dramatically reduced through the implementation of stimulated Raman scattering (SRS) [3,4]. CARS and SRS are coherent Raman spectroscopy (CRS) methods (Fig. 1a) that open the route toward video rate label-free imaging with applications in biology and medical sciences [5,6]. There is a strong demand for CRS endoscopy based on the use of optical fibers, both in basic research where it would permit cellular imaging under conditions in which conventional light microscopy cannot be used, and also for the development of minimally invasive clinical diagnostics and surgical procedures. However, the nonlinear interactions of ultra-short pump pulses with silica fibers have previously prevented the demonstration of CRS in endoscopes [7,8]. As clearly reported in [8], a strong CARS signal is generated in the solid fiber core that necessitates to reject this unwanted radiation before further focalization of the pump and Stokes beams in the sample itself. Although fiber-optic fluorescence imaging with sub-cellular resolution has been demonstrated [9], the need in CRS is to simultaneously deliver two single-mode pump beams with different frequencies and high powers. Furthermore this fiber should collect the generated CRS signal and return it to the fiber input end for analysis. Such a fiber would enable the development of fiber-based CRS imaging systems for use as endoscopes.

Hollow core photonic crystal fibers (HC-PCF) [10] that confine the light in an air core for a restricted range of wavelengths have massively reduced nonlinearity, making them attractive for high peak power laser pulse delivery [11]. However, their use for CRS has two limitations. Firstly, the limited bandwidth means that the spectral range that can be addressed is limited. For example a fiber designed to transmit at 1064 nm will typically have a transmission window spanning approximately only 1800 cm^{-1}. Secondly, the efficiency of collecting and transmitting the CRS signal through the small (few microns) single-mode HC-PCF fiber core is very low. The signal is in any case intrinsically weak as most of the phased matched SRS and CARS signal is emitted in the direction away to the fiber end [12]. Double-clad PCF's with solid cores have been previously demonstrated to significantly enhance the detection efficiency by incorporating a large multimode second cladding [13,14]. Until now, this concept has not been applied to HC-PCF.

In this paper we give a first demonstration of the use of double-clad HC-PCF to perform remote CARS and SRS microscopy in a scheme that is compatible with endoscopy. Both the delivery of the incoming beams (pump and Stokes) and the collected CARS and SRS signals

#146014 - $15.00 USD Received 20 Apr 2011; revised 7 Jun 2011; accepted 7 Jun 2011; published 14 Jun 2011

are transmitted through the same double-clad HC-PCF, the former being confined to the hollow core and the latter being guided in the multimode cladding. Most importantly, and unlike previous works [7,8], no CARS signal is generated in the HC-PCF and the back collection is possible thanks to the fiber double-clad. Although our demonstration makes use of a scanning microscope, the fiber is fully compatible with distal fiber tip scanning endoscope schemes [9].

2. Methods

2.1 Double-clad photonic crystal fiber

Figure 1b shows a scanning electron microscope (SEM) image of the HC-PCF that has been used in this experiment. The central hollow core is surrounded by a photonic crystal cladding which confines the excitation light to the core. The surrounding solid glass annular waveguide guides the generated CRS signal back for analysis. The cross sectional area for signal collection is approximately 2260 μm^2. The width of the air cladding struts supporting the outer core is around 200 nm. The fiber was fabricated from pure fused silica using a multi-stage stack and draw process [15]. The stacked preform was drawn down on a conventional fiber-drawing tower to a final fiber diameter of 103μm. A cut-back measurement was carried out to determine the transmission loss of the hollow-core of the fiber and this is shown in Fig. 1c. The low loss hollow-core transmission window extends from around 950 nm to 1150 nm. Beyond 1150 nm, transmission of light in the hollow core is attenuated, which limits the wavenumber shift to 800 cm^{-1} when all the CARS wavelengths (pump, Stokes and anti-Stokes) are transmitted by the fiber core. However, since the anti-Stokes signal can be collected by the outer waveguide which supports broadband light guidance, the full 1800 cm^{-1} bandwidth can be used in CARS. Indeed, the same bandwidth can be used in SRS. The near field mode profile of the core-guided mode of the fiber is shown in Fig. 1d and is seen to be smooth and single lobed as required for optimal focusing. The fiber supports two orthogonally polarized modes due to form birefringence induced by the core ellipticity and these have been found, through pulse compression experiments, to have group velocity dispersions at 1064 nm of around 110 and 37 ps nm^{-1} km^{-1} respectively.

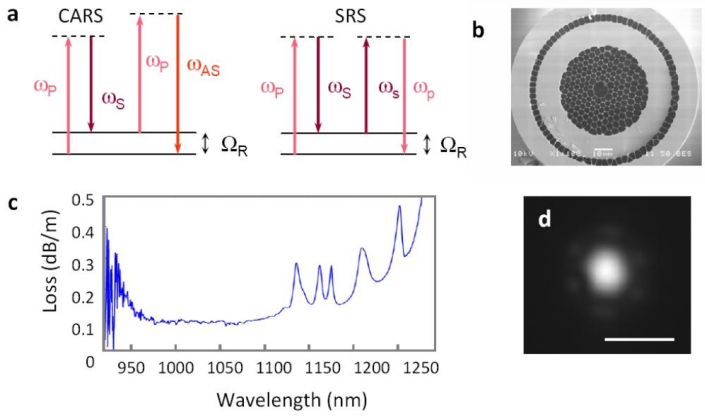

Fig. 1. CRS contrasts and photonic crystal fiber design. (a) Scheme of the CARS and SRS processes, λ_P, λ_S, λ_{AS} stand for the pump, Stokes and anti-Stokes beams respectively and Ω_R for the molecular vibrational resonance. (b) SEM image of the double-clad silica hollow core photonic crystal fiber (HC-PCF). (c) Fiber transmission loss in dB/m. (d) 1064nm near field image confined into the hollow core, Scale bar is 10 μm in figures (b) and (d).

2.2 CRS endoscope like scheme

Figure 2 shows the setup of the experiment. A small fraction of a 76 Mhz, 7 picoseconds mode locked laser (Nd:YVO) emitting at 1064nm is used to generate the Stokes beam with an

#146014 - $15.00 USD Received 20 Apr 2011; revised 7 Jun 2011; accepted 7 Jun 2011; published 14 Jun 2011

output power of 100 mW. The largest fraction of the 1064 nm output power is frequency doubled to synchronously pump an optical parametric oscillator (OPO). In this work the OPO signal beam (tuned between 962 nm and 971 nm), with an output power of 100 mW, is used as the pump beam to perform CARS. The pump and Stokes beams are combined, set into the same linear polarization state, and the temporal delay is adjusted using a dedicated delay line [16]. They are then focused with an aspheric coupling lens into the hollow core of a 1m long piece of double-clad HC-PCF (described above).

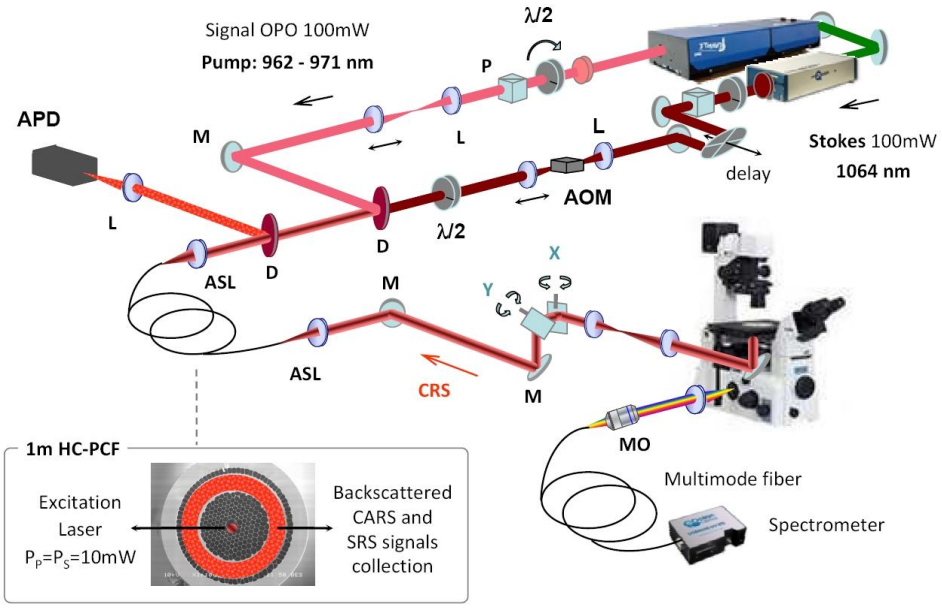

Fig. 2. CARS and SRS experimental setup. APD for avalanche photodiode; M for silver mirrors; P for polarizer; L for NIR achromatic doublets, AOM for acousto-optic modulator and D for dichroic filter. Inset: Excitation pump and Stokes beams are sent into the 5 μm diameter hollow core, Epi and backscattered CARS and SRS signal are collected through the silica double cladding (red ring in SEM fiber picture).

The pump and Stokes beams are re-collimated at the fiber output with an aspheric lens and sent into a custom made inverted scanning microscope [16] with a power of 10mW in each beam. The Epi and backscattered CARS and SRS (pump beam) signals generated at the sample plane are back-coupled into the double-clad HC-PCF and finally detected with an avalanche photodiode (APD – SPCM Perkin Elmer). In the CARS operation mode the anti-Stokes signal is filtered and detected with an APD working in the photon counting regime. In the SRS operation mode the Stokes beam is modulated in amplitude at the frequency of 1MHz thanks to an acousto-optic modulator (see Fig. 2). The stimulated Raman loss (SRL) is detected on the pump beam with an analog APD (Hamamatsu C5460) and a fast lock-in amplifier as reported in [3]. No CARS signal is found to be generated in the HC-PCF when coupling the temporally overlapping pump and Stokes beams into the air core. This is due to the very small overlap of the guided mode with silica of the fiber, which is typically less than 1%. On the contrary, a strong CARS signal has been found in every conventional fiber and solid-core PCF that has been tested. It is a key property of the HC-PCF used here that the sample is illuminated with light that is free of the CARS anti-Stokes wavelength, ensuring that all signal originates only from the sample itself. This situation is unlikely to be found with any other type of fiber. In our experiment the CARS signal is generated between 877 nm and 892 nm and so is outside of the HC-PCF transmission window. This means that the detected CARS signal is transmitted by the air-clad silica annulus surrounding the PCF region. In the SRS operation mode, although the back-reflected pump beam falls into the HC-PCF transmission window, we found that most of the back-guided pump light comes from the

#146014 - $15.00 USD Received 20 Apr 2011; revised 7 Jun 2011; accepted 7 Jun 2011; published 14 Jun 2011

silica annulus (see Fig. 2 inset). Although difficult to quantify experimentally, we estimate the improvement of the back collection efficiency of the order of 50 between the double clad HC-PCF and a conventional single mode fiber.

3. Results and discussion

3.1 CARS spectroscopy on TTB molecular crystal

With these pump and Stokes wavelength settings, and as a proof of principle, we aim at investigating the 990 cm^{-1}-1000 cm^{-1} range for vibrational bond imaging of TTB molecular films crystallized on glass surfaces. 1,3,5-tricyano-2,4,6-tris(p-diethyl-aminostyryl)benzene (TTB) is a nonlinear organic crystal featuring highly conjugated molecules, arranged in a non-centrosymmetric crystalline structure. Furthermore the micron-size TTB crystalline structure makes this molecular crystal interesting for nonlinear microscopy as demonstrated recently in [16] for two-photon excitation fluorescence (TPEF), second harmonic generation (SHG), sum frequency generation (SFG) and four wave mixing (FWM). More interestingly here, TTB crystals also exhibit several vibrational resonances that can be addressed with CRS techniques. Detail of TTB free-cast films synthesis and characterization can be found in [17].

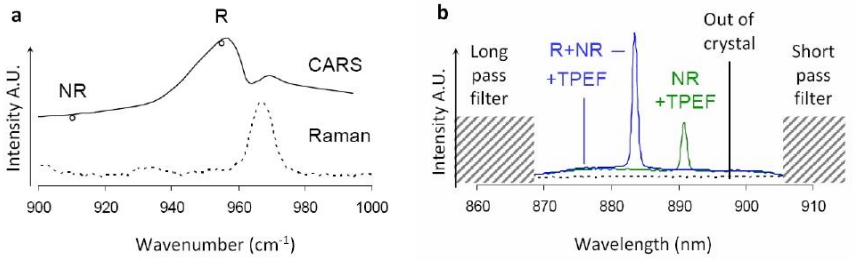

Fig. 3. CARS and spontaneous Raman spectra of TTB crystals. (a) CARS (solid line) and Raman spectra (dashed line) offset for clarity. (b) Spectral response in the resonant CARS situation R + NR + TPEF at 953 cm^{-1} (λp = 966 nm) (blue line) and in the nonresonant resonant NR + TPEF at 915 cm^{-1} (λs = 969.6 nm) (green line). The black dashed line shows the spectral response when the excitation beams are focused out of the crystal (λp = 966 nm - resonant situation). Dashed areas shows the blocking filters used.

Figure 3a shows together the CARS and spontaneous Raman spectra (obtained with a custom made Raman microscope) of TTB crystal in the 900 cm^{-1}-1000 cm^{-1} spectral range. Clearly the 966 cm^{-1} Raman band gives rise to a red-shifted CARS signal around 955 cm^{-1}. Figure 3b shows the CARS spectral features associated with the targeted TTB vibrational resonance. For this experiment the pump and Stokes beam are delivered at the sample plane through the HC-PCF and the CARS signal is detected directly in the Epi direction using a compact spectrometer (see Fig. 2). In the resonant CARS situation (refer as R + NR blue line) at 953 cm^{-1} (λ_p = 966 nm) the spectrum exhibits the sharp CARS peak associated with the resonant (R) and the nonresonant resonant (NR) CARS together with the remaining TPEF inherent to TTB IR excitation. In the nonresonant resonant CARS situation (refer as NR green line) at 915 cm^{-1} (λ_p = 969.6 nm) the spectrum intensity is weaker as being only associated to the nonresonant resonant CARS signal and the TPEF. Also on Fig. 3 is shown the recorded spectrum when the pump and Stokes beams are focused out of the TTB crystal (black dashed line). Clearly, no signal is recorded which further confirms the absence of CARS generated within the HC-PCF.

3.2 CARS endoscope scheme

We now move to the 'endoscope-like' scheme and consider first the CARS process. In this situation, the CARS signal is back coupled into the second cladding of the HC-PCF and detected with the APD detector. We use the scanning mirror to image the spatial features

#146014 - $15.00 USD Received 20 Apr 2011; revised 7 Jun 2011; accepted 7 Jun 2011; published 14 Jun 2011

associated to TTB crystals. These have crystallized in our test sample in dendritic structures. Figure 4 shows two different areas corresponding to a single crystal (Fig. 4a, c, e) and to multiple crystals (Fig. 4b, d, f). For each of the areas are displayed the image taken at resonance (953 cm^{-1}), containing the R, NR and TPEF contributions, together with the image taken off resonance (915 cm^{-1}), containing only the NR and TPEF contributions. From the spectra acquired in Fig. 3 we can safely consider that the resonant CARS signal can be obtained by the simple subtraction between the two images taken at resonance (953 cm^{-1}) and off resonance (915 cm^{-1}). Figure 4e and 4f show the results of this subtraction for the two areas considered and demonstrate the ability of the double-clad HC-PCF to perform CARS imaging in an 'endoscope-like' scheme.

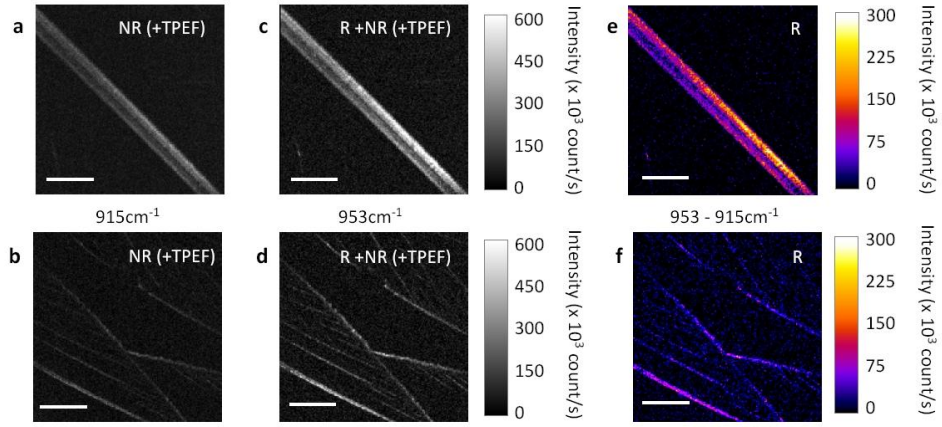

Fig. 4. CARS images of TTB crystals recorded using double-clad HC-PCF fiber for excitation beams delivery and signal collection. (a,b) Nonresonant Resonant CARS situation at 915 cm^{-1} containing TPEF signal (NR + TPEF). (c,d) Resonant CARS situation at 953 cm^{-1} containing the resonant, nonresonant resonant CARS and TPEF (R + NR + TPEF). (e, f) Resonant CARS signal at 953 cm^{-1} obtained with simple subtraction (R + NR + TPEF)-(NR + TPEF). Scale bar is 25 µm. 200 x 200 pixels. 50 µs/pixel, pump and Stokes power: 10mW.

3.3 SRS endoscope scheme

We now consider the SRS process where we modulate the Stokes beam and detect the stimulated Raman loss (SRL) on the pump beam. In a conventional solid core fiber SRS is always present due to four wave mixing in the fiber core itself [18]. Similar to the CARS scheme, no SRL modulation is present when the propagation of the pump and Stokes beams takes place in the HC-PCF. Note that in the SRS experiments, and for software control reasons, we do not use the scanning mirrors but raster scan the sample with an *xy* piezo stage. Figure 5 shows a nonresonant resonant image taken at 915cm^{-1} (Fig. 5a) and a resonant image taken at 968cm^{-1} (Fig. 5 b) corresponding to the peak of the Raman targeted line (see Fig. 3a). As in the case of CARS, there is no SRS signal detected when the active spot is located out of the crystal confirming the absence of SRS signal in the HCF-PCF itself. Although the resonant image (968cm^{-1}) exhibits a strong signal that reproduces the Raman spectrum (see Fig. 5d), there remains an SRL contribution far from resonance that is visible in Fig. 5a and as a plateau in the SRL spectrum of Fig. 5d. We attribute this nonresonant resonant depletion to nonlinear processes in the TTB crystal itself. Although Kerr lens effects due to pump and Stokes crossed phase modulation cannot be discarded, we believe that most of the nonresonant resonant pump depletion comes from sum frequency generation (SFG). Indeed, SFG is found to be very strong in these TTB crystals, originally designed to exhibit strong second order nonlinearities (data not shown). In principle SRS imaging would require a simple HC-PCF, without the double-clad, with the pump and Stokes beams falling in its transmission window. This would be very challenging because the back coupling efficiency of the scattered pump beam into the small single-mode hollow core is extremely weak. In the

#146014 - $15.00 USD Received 20 Apr 2011; revised 7 Jun 2011; accepted 7 Jun 2011; published 14 Jun 2011

present SRS experiment, the air-clad silica annulus collects most of the retro-reflected pump light. Although the double-clad HC-PCF provides a very attractive way of performing CRS in endoscopes, there is still need to improve the back coupling efficiency that is estimated here to be, at most, 10% of the backscattered CARS signal (as compared to a nondescanned detection). This is mainly due to the descanned detection scheme that restricts the back detection within the fiber. We believe that this could be improved by thermally collapsing the PCF cladding at the fiber tip whilst allowing the hollow core to remain open. This would have the effect of both increasing the collection area of the fiber and bringing the collection area closer to the center of the back focal plane of the distal optics at which point the signal should be brightest. Increased efficiency could also be obtained through careful consideration and engineering of the achromaticity and numerical aperture of the optics that are used to simultaneously carry out two very different tasks.

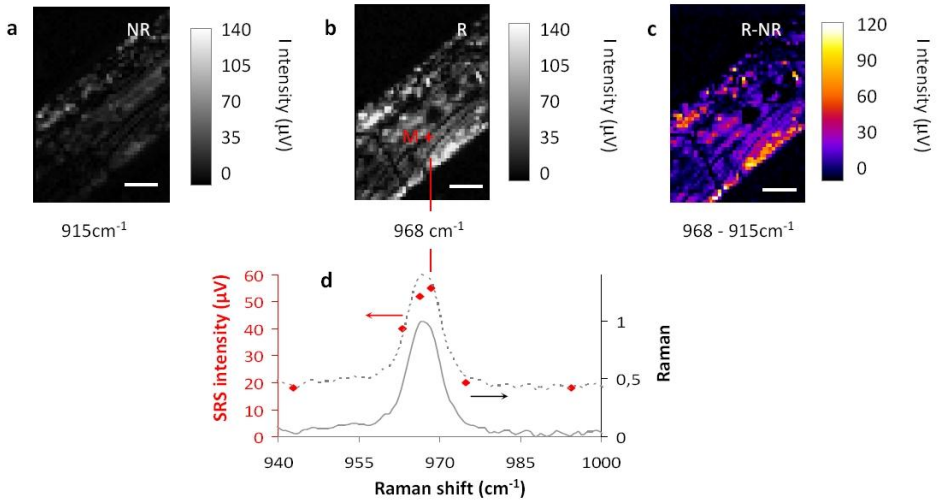

Fig. 5. SRS images of TTB crystals recorded using double-clad HC-PCF fiber for excitation beams delivery and signal collection. (a) Nonresonant Resonant SRS situation at 915 cm^{-1} (NR). (b) Resonant SRS situation at 968 cm^{-1} (R). (c) Direct subtraction (R-NR). (d) SRS spectrum (♦) taken for point M in (b) and normalized Raman spectrum (solid line). The dashed line is the Raman spectrum that has been offset and superimposed to the SRS measured points. Scale bar is 10 µm. 45 x 60 pixels. 50 ms/pixel, pump and Stokes power: 10mW.

4. Conclusion

We have demonstrated that double-clad hollow-core photonic crystal fibers are suitable to perform coherent Raman spectroscopic imaging in an 'endoscope-like' scheme. Both CARS and SRS processes have been considered. The key features of these fibers are (1) that no wave mixing signals are generated within the fiber for temporally overlapping pulses and (2) that the air-clad signal return annulus enables both the spectral range for nonlinear microscopies to be greatly extended and the back coupling efficiency of the signal to be greatly improved. Although the implementation reported here is far from an endoscope featuring a compact focusing unit, the presented double-clad HC-PCF is fully compatible with a distal fiber tip scanning endoscope scheme [9]. We believe that such fibers and their forthcoming development to be suitable for spectroscopy and video rate imaging [18] in CRS endoscopes.

Acknowledgements

We thank Prof. Bong Rae Cho and Dr. Mi-Yun Jeong for synthesizing the TTB crystalline films and Dr. Sophie Brasselet for preliminary SHG studies on these films, Dr. Jérôme Wenger and Andreas Volkmer for fruitful discussions. We acknowledge financial support from the French Ministry of Research, the CNRS, and the European Union (grant CARSExplorer FP7 Health).

#146014 - $15.00 USD Received 20 Apr 2011; revised 7 Jun 2011; accepted 7 Jun 2011; published 14 Jun 2011